Three-dimensional graphene based passively mode-locked fiber laser

Y. Yang[#], M. Loeblein[#], S. H. Tsang, K. K. Chow[*], and E. H. T. Teo

School of Electrical and Electronic Engineering, Nanyang Technological University,
50 Nanyang Avenue, Singapore 639798
[#]Equal contributions
[*]kkchow@ntu.edu.sg

Abstract: We present an all-fiber passively mode-locked fiber laser incorporating three-dimensional (3D) graphene as a saturable absorber (SA) for the first time to the best of our knowledge. The 3D graphene is synthesized by template-directed chemical vapor deposition (CVD). The SA is then simply formed by sandwiching the freestanding 3D graphene between two conventional fiber connectors without any deposition process. It is demonstrated that such 3D graphene based SA is capable to produce high quality mode-locked pulses. A passively mode-locked fiber laser is constructed and stable output pulses with a fundamental repetition rate of ~9.9 MHz and a pulse width of ~1 ps are generated from the fiber laser. The average output power of the laser is ~10.5 mW while the output pulse is operating at single pulse region. The results imply that the freestanding 3D graphene can be applied as an effective saturable absorption material for passively mode-locked lasers.

OCIS codes: (060.3510) Laser, fiber; (160.4330) Nonlinear optical materials; (140.4050) Mode-locked lasers.

References and links

1. L. E. Nelson, D. J. Jones, K. Tamura, H. A. Haus, and E. P. Ippen, "Ultrashort-pulse fiber ring lasers," Appl. Phy. B **65**, 277 - 294 (1997).
2. M. E. Fermann, and I. Hartl, "Ultrafast fiber laser technology," IEEE J. Sel. Top. Quantum Electron. **15**, 191-206 (2009).
3. V. J. Matsas, T. P. Newson, D. J. Richardson, and D. N. Payne, "Selfstarting passively mode-locked fibre ring soliton laser exploiting nonlinear polarisation rotation," Electron. Lett. **28**, 1391-1393 (1992).
4. O. Okhotnikov, A. Grudinin, and M. Pessa "Ultrafast fiber systems based on SESAM technology: New horizons and applications," New J. Phys. **6**, 177(2004).
5. D. Y. Tang, H. Zhang, Q. L. Bao, and K. P. Loh, "Graphene mode locked ultrafast fiber lasers," in *Fiber Lasers VIII: Technology, Systems, and Applications,* Proc. SPIE 7914, 79141H (2011).
6. U. Keller, "Recent developments in compact ultrafast lasers," Nat. **424**, 831-838 (2003).
7. A. Martinez, and Z. Sun, "Nanotube and graphene saturable absorbers for fiber laser, " Nat. Photonics **7**, 842–845 (2013).
8. Z. Sun, T. Hasan, and A. C. Ferrari, "Ultrafast lasers mode-locked by nanotubes and graphene," Physica E **44**, 1082-1091 (2012).
9. S. Yamashita, "A tutorial on nonlinear photonic applications of carbon nanotube and graphene," J. Lightw. Technol. **30**, 427-447 (2012).
10. F. Bonaccorso, Z. Sun, T. Hasan, and A.C. Ferrari, "Graphene photonics and optoelectronics," Nat. Photonics **4**, 611-622(2010).
11. F. Bonaccorso, A. Lombardo, T. Hasan, Z. Sun, L. Colombo, and A. C. Ferrari, "Production and processing of graphene and 2d crystals, " Mater. Today **15**, 564-589 (2012).
12. A. K. Geim, and K. S. Novoselov, "The rise of graphene," Nat. Mater. **6**, 183-191 (2007).
13. Y. W. Song, S. Y. Jang, W. S. Han, and M. K. Bae, "Graphene mode-lockers for fiber lasers functioned with evanescent field interaction. " Appl. Phys. Lett. **96**, 051122 (2010).

14. Q. L. Bao, H. Zhang, Y. Wang, Z. H. Ni, Y. L. Yan, Z. X. Shen, K. P. Loh, and D. Y. Tang, "Atomic-layer graphene as a saturable absorber for ultrafast pulsed lasers," Adv. Funct. Mater. **19**, 3077-3083 (2009).
15. Z. Sun, T. Hasan, F. Torrisi, D. Popa, G. Privitera, F. Wang, F. Bonaccorso, D. M. Basko, and A. C. Ferrari, "Graphene mode-locked ultrafast laser," ACS Nano. **4**, 803-810 (2010).
16. A. A. Lagatsky, Z. Sun, T. S. Kulmala, R. S. Sundaram, S. Milana, F. Torrisi, O. L. Antipov, Y. Lee, J. H. Ahn, C. T. A. Brown, W. Sibbett, and A. C. Ferrari, "2 μm solid-state laser mode-locked by single-layer graphene," Appl. Phys. Lett. **102**, 013113 (2013).
17. R. Mary, G. Brown, S. J. Beecher, F. Torrisi, S. Milana, D. Popa, T. Hasan, Z. Sun, E. Lidorikis, S. Ohara, A. C. Ferrari, and A. K. Kar, "1.5 GHz picosecond pulse generation from a monolithic waveguide laser with a graphene-film saturable output coupler," Opt. Express **21**, 7943-7950 (2013).
18. S. Husaini, and R. G. Bedford, "Graphene saturable absorber for high power semiconductor disk laser mode-locking," Appl. Phys. Lett. **104**, 161107 (2014) **.**
19. D. Popa, Z. Sun, F. Torrisi, T. Hasan, F.Wang, and A. C. Ferrari, "Sub 200 fs pulse generation from a graphene mode-locked fiber laser," Appl. Phys. Lett. **97**, 203106 (2010).
20. B. Fu, Y. Hua, and X. Xiao, "Broadband graphene saturable absorber for pulsed fiber laser at 1, 1.5, and 2μm," IEEE J. Sel. Top. Quantum Electron. **20**, 1100705(2014).
21. V. H. Pham, T. V. Cuong, S. H. Hur, E. W. Shin, J. S. Kim, J. S. Chung, and E. J. Kim, "Fast and simple fabrication of a large transparent chemically-converted graphene film by spray-coating," Carbon **48**, 1945-1951 (2010).
22. H. Kim, J. Cho, S. Y. Jang, and Y. W. Song, "Deformation-immunized optical deposition of graphene for ultrafast pulsed lasers," Appl. Phys. Lett. **98**, 021104 (2011).
23. A. Martinez, K. Fuse1 and S. Yamashita, "Mechanical exfoliation of graphene for the passive mode-locking of fiber lasers," Appl. Phys. Lett. **99**, 121107 (2011).
24. Z. Chen, W. Ren, L. Gao, B. Liu, S. Pei, and H. M. Cheng, "Three-dimensional flexible and conductive interconnected graphene networks grown by chemical vapour deposition," Nat. Mater. **10**, 424-428 (2011).
25. J. S. Lee, H. J. Ahn, J. C. Yoon, and J. H. Jang, "Three-dimensional nano-foam of few-layer graphene grown by CVD for DSSC," Phys. Chem. Chem. Phys. **14**, 7938-7943 (2012).
26. M. Loeblein, R. Y. Tay, S. H. Tsang, W. B. Ng, and E. H. T. Teo, "Configurable three-dimensional boron nitride–carbon architecture and its tunable electronic behavior with stable thermal performances," Small **10**, 2992-2999 (2014).
27. A. Reina, X. Jia, J. Ho, D. Nezich, H. Son, V. Bulovic, M. S. Dresselhaus, and J. Kong, "Large area, few-layer graphene films on arbitrary substrates by chemical vapor deposition," Nano Lett. **9**, 30-35 (2008).
28. S. J. Chae, F. Güneş, K. K. Kim, E. S. Kim, G. H. Han, S. M. Kim, H. J. Shin, S. M. Yoon, J. Y. Choi, M. H. Park, C. W. Yang, D. Pribat, and Y. H. Lee, "Synthesis of large-area graphene layers on poly-nickel substrate by chemical vapor deposition: wrinkle formation," Adv. Mater **21**, 2328-2333 (2009).
29. A. C. Ferrari, J. C. Meyer, V. Scardaci, C. Casiraghi, M. Lazzeri, F. Mauri, S. Piscanec, D. Jiang, K. S. Novoselov, S. Roth, and A. K. Geim, "Raman spectrum of graphene and graphene layers," Phys. Rev. Lett. **97**, 187401 (2006).
30. M. Pimenta, G. Dresselhaus, M. S. Dresselhaus, L. Cancado, A. Jorio, and R. Saito, "Studying disorder in graphite-based systems by Raman spectroscopy," Phys. Chem. Chem. Phys. **9**, 1276-1290 (2007).
31. P. A. Obraztsov, M. G. Rybin, A. V. Tyurnina, S. V. Garnov, E. D. Obraztsova, A. N. Obraztsov, and Y. P. Svirko, "Broadband light-induced absorbance change in multilayer graphene," Nano Lett., **11** , 1540–1545(2011).
32. Y. Zhao, X. Li, M. Xu, H. Yu, Y. Wu, Z. Wang, X. Hao, and X. Xu, "Dual-wavelength synchronously Q-switched solid-state laser with multi-layered graphene as saturable absorber," Opt. Express **21**, 3516-3522(2013).
33. H. Baek, H. W. Lee, S. Bae1, B. H. Hong, Y. H. Ahn, D. I. Yeom and F. Rotermund, "Efficient mode-locking of sub-70-fs Ti:sapphire laser by graphene saturable absorber," Appl. Phys. Express **5**, 032701 (2012).
34. S. D. Di Dio Cafiso, E. Ugolotti, A. Schmidt, V. Petrov, U. Griebner, A. Agnesi, W. B. Cho, B. H. Jung, F. Rotermund, S. Bae, B. H. Hong, G. Reali, and F. Pirzio, "Sub-100-fs Cr:YAG laser mode-locked by monolayer graphene saturable absorber, " Opt. Lett. **38**, 1745-1747 (2013).
35. P. L. Huang, S. C. Lin, C. Y. Yeh, H. H. Kuo, S. H. Huang, G. R. Lin, L. J. Li, C. Y. Su, and W. H. Cheng, "Stable mode-locked fiber laser based on CVD fabricated graphene saturable absorber," Opt. Express **20**, 2460-2465(2012).
36. Y. W. Song, K. Morimune, S. Y. Set, and S. Yamashita, "Polarization insensitive all- fiber mode-lockers functioned by carbon nanotubes deposited onto tapered fibers," Appl. Phys. Lett. **90**, 021101 (2007).

1. Introduction

Passively mode-locked lasers capable of generating ultra-short optical pulses have attracted considerable attentions for the number of potential applications ranging from basic research to sensing, high speed optical communication, supercontinuum generation, medicine and material processing depending on the operation wavelength and pulse width [1]. In particular, all-fiber passively mode-locked laser owns advantages of simple and compact design, high peak power, excellent beam quality, high power conversion efficiency, low cost and reliability [2]. To achieve passively mode-locking in a fiber laser by incorporating saturable absorbers (SAs), conventionally there are several different technologies including nonlinear polarization rotation (NPR) [3] and discrete SAs [4]. The NPR technique is based on the light interference in a laser cavity which functions as an artificial SA [5]. However, since light interference is sensitive to phase change, mode-locking of fiber lasers by NPR technique is relatively unstable due to environmental perturbation. An alternative method to strengthen the laser robustness is to apply semiconductor saturable absorber mirrors (SESAMs). SESAMs are complex quantum well devices fabricated by molecular beam epitaxy on distributed Bragg reflectors [4, 6]. However, SESAMs have complex fabrication process and limited operation bandwidth. Such limitations motivate research on new materials for SAs.

Graphene has been demonstrated as a strong candidate for SAs which offers many significant advantages including intrinsic broadband operation from ultraviolet to the far-infrared region [7], ultrafast recovery time, and high thermal damage threshold [5-9]. Graphene was conventionally fabricated by the mechanical exfoliation method in 2004 and since then various kinds of preparation methods are intensively explored [10-12]. Graphene based SAs have been successfully implemented in a variety of lasers including fiber lasers [13-15], solid-state lasers [16], waveguide lasers [17] and semiconductor lasers [18]. Since Bao *et al.* and Sun *et al.* have demonstrated in [14, 15], mode-locked fiber lasers incorporating graphene as SAs have attracted considerable attention and have been actively explored. Recently, Popa *et al.* have demonstrated generation of 174 fs pulses from a graphene based erbium-doped fiber laser [19], and Fu *et al.* reported up to 1000 nm broadband ultrafast pulse generation from several different fiber lasers mode-locked by the same graphene based SA [20]. In order to fabricate a graphene based SA to be inserted into a laser cavity to interact with propagating light, several approaches have been demonstrated for the fabrication of the graphene based SA such as spray coating method [21], optically-driven deposition method [22], direct mechanical exfoliation and imprinted graphite nano-particle method [23], CVD graphene film transferred by de-ionized (DI) water floating and dipping method [5]. However, it is difficult to control the number of graphene layers that needs to be transferred to the fiber connector end precisely when using the first three methods, and hence the performance of the prepared SAs is hard to estimate. Additionally, the first two methods require an extra procedure to prepare graphene based solution. The last method of CVD graphene film transferred to fiber connector end involves a process of floating and transferring graphene thin film in DI water and drying procedure. During the transfer process of the graphene layers to the fiber connector end facets, the mechanical exfoliation method and CVD graphene film method hold a possibility of damaging the graphene structure.

As the fabrication methods and applications of graphene are actively explored, integration of individual two-dimensional graphene sheets into a macroscopic structure becomes more and more essential for the applications of graphene [24]. 3D graphene is a foam-like structure that consists of multiple graphene layers integrated as a whole. In contrast to graphite, 3D graphene is obtained from bottom-up approach through CVD method. By carefully controlling the growth mechanism, the number of layers and crystallinity can be easily controlled and result in a highly flexible and transparent structure [24], which is ideal for photonics applications. A series of graphene based composites and microstructures have been fabricated using various methods such as chemically derived graphene sheets or direct

synthesis of 3D graphene macrostructure by template-directed CVD. The latter method enables the fabrication of an interconnected flexible network of graphene as the fast transport channel of charge carriers for high electrical conductivity [24, 25]. The fabrication advantage of 3D graphene relies in the free-standing structures obtained. In contrast to graphene films, which often require to be handled with a substrate as a support, this foam-like structures are easier to handle and can be produced uniformly in large scale. In this work, we report on a new type of SA for the passive mode-locking of fiber lasers with simple fabrication method. We demonstrate that 3D graphene can be used as a SA to mode-lock fiber lasers. A 3D graphene based SA is easy to fabricate without any additional deposition procedure because of its freestanding, flexible and elastic network structure. In addition, simple sandwiching of freestanding 3D graphene in between two fiber connectors to form a 3D graphene based SA successfully prevents the possible damage of the saturable absorption material during the SA fabrication process. In this paper, we obtained 3D graphene through a direct synthesis method, characterized the optical properties of 3D graphene and sandwiched the freestanding 3D graphene thin film between two optical fiber connectors to be used as a SA in a mode-locked fiber ring laser. For the first time, to the best of our knowledge, we demonstrate a 3D graphene SA to generate stable ultra-short soliton pulses in a mode-locked erbium-doped fiber laser. We believe that by varying and optimizing the number of graphene layers of the 3D graphene, the saturation absorption strength can be modulated over a wide range to obtain optical pulses with shorter pulse width.

2. Synthesis and characterization of 3D graphene

The 3D graphene (few layers) macrostructure was obtained through a direct synthesis method using template-directed CVD [26]. The growth of 3D graphene was carried out in a split tube (quartz) furnace using Cu foam as a catalytic substrate. The substrate was first annealed at 1000^{o}C. Afterwards ethanol was bubbled into the quartz tube under constant Ar and H_2 flow, which would allow the decomposition of the ethanol to synthesize graphene film on the surface of the Cu foam [27, 28]. Next, the as-grown 3D-C/Cu sample was dip-coated with poly (methyl methacrylate) (PMMA) as a protective layer for the 3D graphene structure and subsequently immersed into hot diluted nitric acid (HNO_3) for 5 hours to completely etch off the Cu supporting structure. The result is a freestanding, ultra-light weight and flexible graphene foam, consisting of a few layers of foam-like graphene in a network, allowing charge carriers to move rapidly and with small resistance through the high-quality and continuous graphene building blocks.

The scanning electron microscopy (SEM) images of each stage of the growth process are shown in Fig. 1(a) and the optical image of the 3D graphene is shown in Fig. 1(b). The structure of the freestanding 3D graphene can be seen to closely resemble that of the Cu foam with a porosity of 99.6% with pore diameter ranging approximately from 100 μm to 200 μm. Fig. 1(c) shows the transmission electron microscopy (TEM) result of the obtained 3D graphene, the average number of layers of the 3D graphene is between 3-7 layers. Fig. 1(d) shows the obtained Raman spectrum for the few-layer 3D graphene. There are three peeks, namely the 2D peak at 2700 cm^{-1}, the G peak at 1580 cm^{-1} and D peak at 1350 cm^{-1} [29]. The G band originates from in-plane vibration of sp^2 carbon atoms; the 2D band originates from a two phonon double resonance Raman process and is also denominated as the second-order Raman band; the D peak is reported to stand for the defect rate of graphene [30]. In the present case, the D peak originates in the very thin character of the samples and small domain sizes, which yield a random orientation of the graphene crystals.

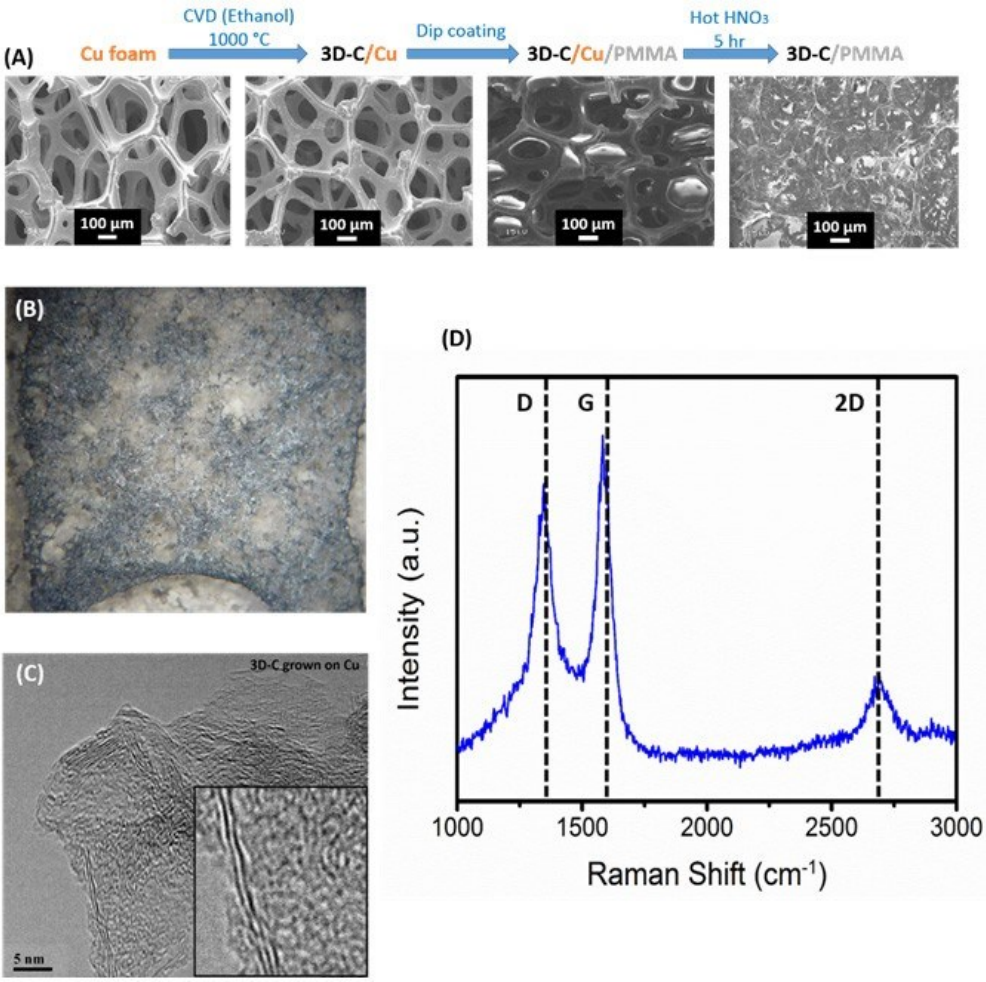

Fig. 1. Characterization of 3D graphene showing (a) the scanning electron microscopy (SEM) images of each state of the growth, (b) the optical image of 3D graphene with 1.8x magnification, (c) the transmission electron microscopy (TEM) image with an average number of layers of 3-7, and (d) the Raman spectrum of the few-layer graphene foam.

The linear transmittance spectrum of the 3D graphene sample was further measured by an UV-Visible-NIR spectrophotometer (Perkin-Elmer Lambda 950). The result shows a wavelength independent absorption over a wide spectral range from 500 to 2200 nm, which is similar to that of graphene. The average optical transmittance between 500 and 2200 nm is ~82% as it is shown in Fig. 2(a). The absorption properties of the 3D graphene are found comparable to those of multi-layer CVD graphene [31, 32]. A femto-second pulsed laser was then applied as the light source to characterize the nonlinear absorption of the prepared 3D graphene based SA. The maximum output power of the pulsed laser was ~9.5 mW at a center wavelength of 1561.9 nm. The output pulse trains exhibited a repetition rate of ~67.1 MHz with a pulse width of ~440 fs. A variable attenuator was connected to the home-built pulsed laser output to tune the output power of the laser. A 90/10 coupler was connected after the attenuator where 10% of the power was coupled to the power meter as a reference power, and 90% of the power was coupled through the 3D graphene based SA and monitored by another power meter. The output power levels, with and without the SA, were measured

simultaneously. Fig. 2(a) shows the transmittance of the 3D graphene material, while Fig. 2(b) shows that of the nonlinear absorption of the 3D graphene based SA. As the measurement in Fig. 2(b) is with respect to the whole SA rather than just the material, the results show a higher background loss. Our 3D graphene based SA shows a modulation depth of ~3.2%, a saturation intensity of ~50 MW/cm^2, and a non-saturable loss of ~43.7%, as shown in Fig. 2(b). It has been reported that the modulation depth of single-layer CVD graphene is ~1% with a non-saturable loss of ~1.9% [33-34]. Furthermore, the modulation depth of graphene based SAs can be increased by stacking multiple layers of graphene [7]. A 21-layer graphene based SA fabricated through CVD was reported to have a modulation depth of ~2.93%, a saturation intensity of ~53.25 MW/cm^2, and a non-saturable loss of ~53.05% [35]. Our fabricated 3D graphene based SA shows comparable optical properties to that of multi-layer CVD graphene based SAs.

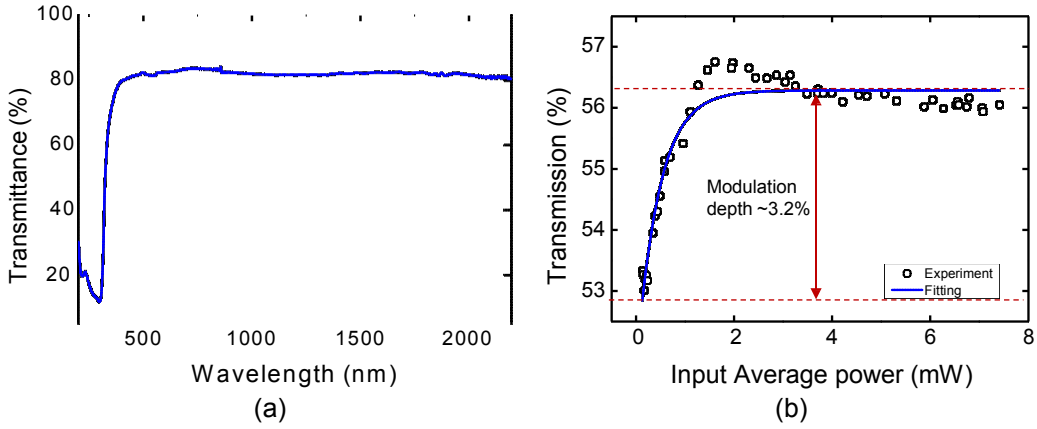

Fig. 2. (a) Transmission spectrum of the 3D graphene measured by a spectrophotometer, and (b) the nonlinear transmission measured by a femto-second pulsed laser.

3. All-fiber ring cavity mode-locked laser setup

A 1.55-μm ring cavity passively mode-locked fiber laser was further constructed to investigate the performance of the fabricated 3D graphene based SA as shown in Fig. 1. The fabricated 3D graphene was cut to ~2 mm × 2 mm in size in preparation process. And the 3D graphene based SA was prepared by direct placed freestanding 3D graphene between two FC/APC fiber connector end facets through a conventional adapter. The prepared device was then used as a SA in the mode-locked erbium-doped fiber laser cavity. Fig. 3 shows the ring cavity passively mode-locked fiber laser setup incorporating the prepared 3D graphene based SA. The total length of the laser cavity was estimated to be ~20.9 m. A 0.6 m long erbium-doped fiber (nLight LIEKKI Er110-4/125) with group velocity dispersion parameter β_2 of 0.012 ps^2/m and peak core absorption of 110 dB/m at 1530 nm was used as the gain medium in the laser cavity. The other fibers were all standard single mode fibers with a length of ~20.3 m. A 980/1550 nm single mode wavelength-division multiplexer (WDM) coupler was used to launch a 980 nm pump light into the laser cavity, where an polarization-independent isolator (ISO) was applied to ensure the unidirectional light propagation in the laser cavity. A polarization controller (PC) was employed to adjust the cavity polarization and optimize the mode-locking condition in the cavity. 50% of the optical power at the emission wavelength was coupled out as the laser output from the laser cavity by a 1 × 2 optical coupler. The total cavity dispersion β_2 was managed in the anomalous region with -0.42 ps^2 for soliton shaping. The characteristics of the output pulses including the optical spectrum, the repetition rate and

the pulse width were observed using an optical spectrum analyzer (Ando AQ6317B), a 2GHz photo-detector (Thorlabs DET01CFC) followed by a signal source analyzer (Rohde & Schwarz FSUP26), and an autocorrelator (Alnair Labs HAC-200), respectively.

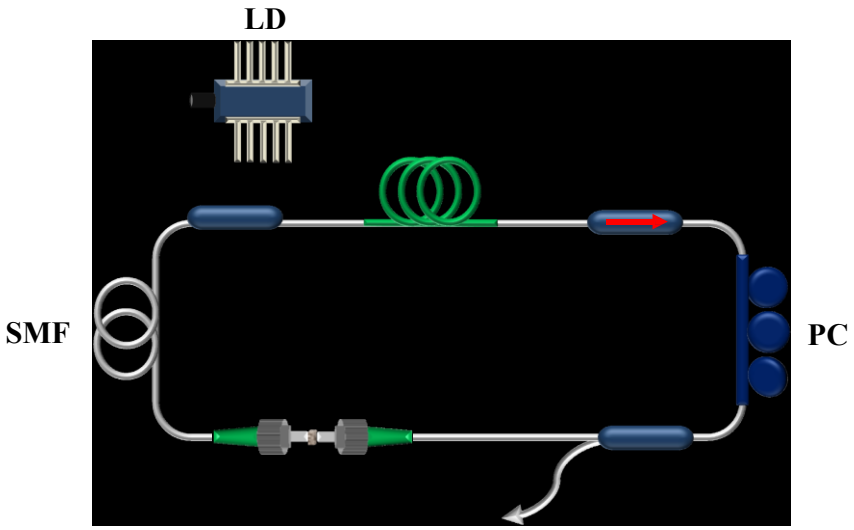

Fig. 3. Schematic of all-fiber ring laser mode-locked by 3D graphene based SA. LD: pump laser diode; WDM: wavelength-division multiplexer; EDF: erbium-doped fiber; ISO: isolator; PC: polarization controller; OC: output coupler; SA: 3D graphene based saturable absorber; SMF: single mode fiber.

4. Experimental results and discussion

In the experiment, when the pump power was increasing up to ~35.6 mW, continuous wave lasing was observed with an appropriate PC setting. The pump power threshold for single-soliton generation was found to be ~130.03 mW. Self-started mode-locking was also observed. To achieve a single soliton with a relatively high output power, the pump power was further increased to ~135.1 mW. The spectrum of the soliton pulses is shown in Fig. 4(a), where the center wavelength is located at 1561.4 nm and the 3-dB spectral bandwidth is ~2.3 nm. The autocorrelation trace of the output pulse was measured to be ~1.01 ps with a sech^2 pulse shape fitting as shown in Fig. 4(b), where the solid red line is the sech^2 pulse fitting and the black circles are the experimental data. Fig. 4(c) shows the radio frequency (RF) spectrum of the output pulses for the fundamental repetition rate which corresponds to the laser cavity length, and the fundamental peak corresponds to the cavity repetition rate of ~9.9 MHz; the signal to noise ratio of the fundamental repetition rate is larger than 80 dB above the noise level, indicates that stable soliton pulses were being generated. The wideband RF spectrum to show the pulse train of ~9.9 MHz repetition rate of the mode-locked pulses is given in Fig. 4(d). The laser average output power coupled out through a 50% coupler from the laser cavity was found to be ~10.5 mW while the pump power was set at ~135.1 mW. Therefore, the output pulse energy was estimated ~1 nJ for single pulse operation of the mode-locked laser. The output power of the constructed fiber laser is believed to be limited by the damage threshold of the 3D graphene based SA. One further improvement could be utilizing evanescent-field interaction of the propagating light and the 3D graphene, which could be realized by using side-polished fibers [13] or tapered fibers [36] together with the 3D graphene to form the SA. The laser operation for soliton pulse generation was found to be stable. We also measured the stability of the laser output, negligible variation of the laser

output parameters was observed over several hour periods of operation. When the 3D graphene based SA is removed from the laser cavity, mode-locking operation was found to be impossible even with a further increase in the pump power to ~200 mW. This observation confirms that the SA provides the required mechanism to initiate and sustain the passive mode-locking operation, where the 3D graphene is the key component.

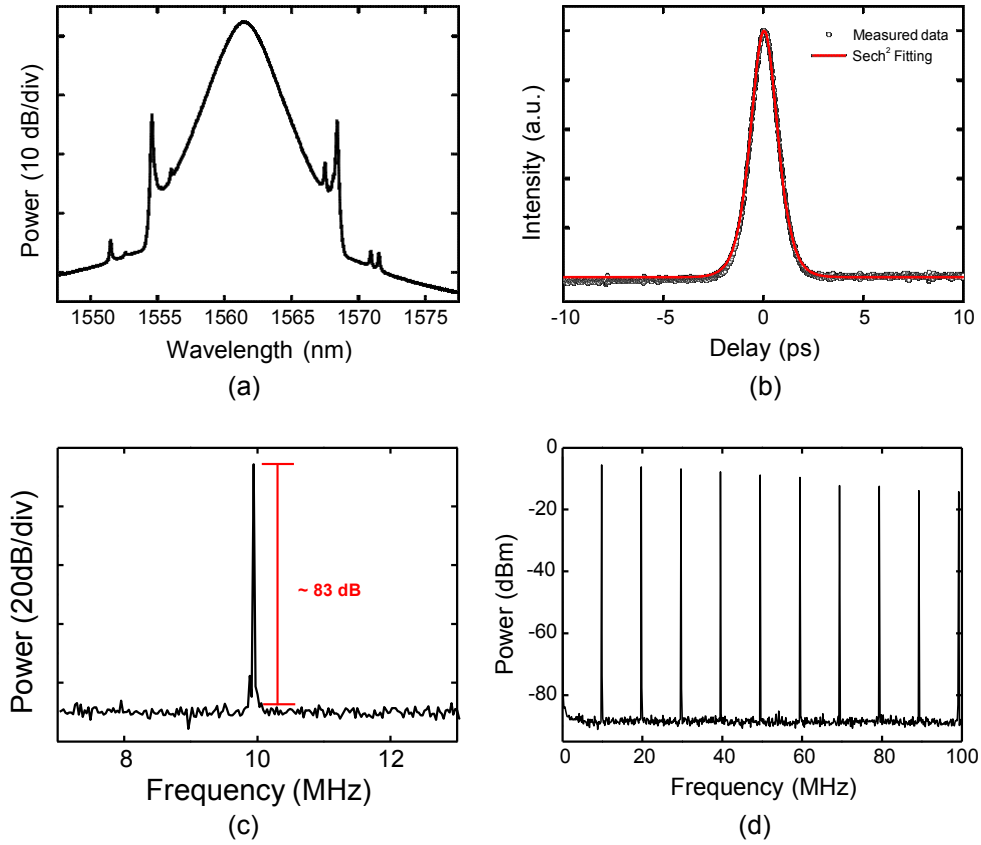

Fig. 4. Characteristics of the output of the fiber laser showing (a) the optical spectrum, (b) the autocorrelation trace, (c) the fundamental RF spectrum, and (d) the wideband RF spectrum.

5. Conclusion

In summary, we report that 3D graphene can exhibit saturation absorption. We have presented a simple, convenient method to form 3D graphene based SAs to generate high power and stable ultra-short pulses. Self-starting mode-locked lasing was observed, and the resultant pulse train with a fundamental repetition rate of ~9.9 MHz and a pulse width of ~1.01 ps was achieved. The average output power of the laser was found to be ~10.5 mW with corresponding output pulse energy of ~1 nJ for single pulse operation. Such a freestanding 3D graphene offers a new solution to high quality SAs for fiber lasers with relatively simple and cost effective fabrication process.

Acknowledgments

This work was partially supported by Academic Research Fund Tier 2 Grant (ARC26/14) of Ministry of Education (MOE), Singapore.